



**HAL**  
open science

## Surface functionalization of cyclic olefin copolymer by plasma-enhanced chemical vapor deposition using atmospheric pressure plasma jet for microfluidic applications

Samantha Bourg, Sophie Griveau, Fanny d'Orlyé, Michael Tatoulian, Fethi Bedioui, Cédric Guyon, Anne Varenne

### ► To cite this version:

Samantha Bourg, Sophie Griveau, Fanny d'Orlyé, Michael Tatoulian, Fethi Bedioui, et al.. Surface functionalization of cyclic olefin copolymer by plasma-enhanced chemical vapor deposition using atmospheric pressure plasma jet for microfluidic applications. *Plasma Processes and Polymers*, 2019, 16 (6), pp.1800195. 10.1002/ppap.201800195 . hal-02159787

**HAL Id: hal-02159787**

**<https://hal.science/hal-02159787>**

Submitted on 20 Jul 2019

**HAL** is a multi-disciplinary open access archive for the deposit and dissemination of scientific research documents, whether they are published or not. The documents may come from teaching and research institutions in France or abroad, or from public or private research centers.

L'archive ouverte pluridisciplinaire **HAL**, est destinée au dépôt et à la diffusion de documents scientifiques de niveau recherche, publiés ou non, émanant des établissements d'enseignement et de recherche français ou étrangers, des laboratoires publics ou privés.

1 <sup>2</sup> ((please add journal code and manuscript number, e.g., DOI: 10.1002/ppap.201100001))

2 **Article type: Full paper**

3  
4 **Surface Functionalization of Cyclic Olefin Copolymer by Plasma-Enhanced**  
5 **Chemical Vapor Deposition using Atmospheric Pressure Plasma Jet for**  
6 **Microfluidic Applications**

7  
8  
9 Samantha Bourg, Sophie Griveau, Fanny d'Orlyé, Michael Tatoulian, Fethi Bedioui, Cédric  
10 Guyon\*, Anne Varenne\*

11  
12 \_\_\_\_\_  
13  
14 Samantha Bourg, Dr. Sophie Griveau, Dr. Fanny d'Orlyé, Dr. Féthi Bedioui, Prof. Anne  
15 Varenne\*

16 Chimie ParisTech PSL, CNRS FRE 2027, Institute of Chemistry for Life and Health  
17 Sciences, 11 rue Pierre et Marie Curie, 75005 Paris, France

18 E-mail: [anne.varenne@chimieparistech.psl.eu](mailto:anne.varenne@chimieparistech.psl.eu)

19  
20 Prof. Michael Tatoulian, Dr. Cédric Guyon\*

21 2PM (Plasma processes, Microsystems group) IRCP, Chimie ParisTech PSL, CNRS 8247, 11  
22 rue Pierre et Marie Curie, 75005 Paris, France

23 E-mail: [cedric.guyon@chimieparistech.psl.eu](mailto:cedric.guyon@chimieparistech.psl.eu)

24  
25  
26 \_\_\_\_\_  
27 Lab-On-A-Chips promise solutions for high throughput and specific analysis for environment  
28 and health applications, with the challenge to develop materials allowing fast, easy and cheap  
29 microfabrication and efficient surface treatment. Cyclic Olefin Copolymer (COC) is a  
30 promising thermoplastic, easily microfabricated for both rapid prototyping and low-cost mass  
31 production of microfluidic devices, but still needing efficient surface modification strategies.  
32 This study reports for the first time the optimization of an easy COC silica coating process by  
33 Plasma-Enhanced Chemical Vapor Deposition at Atmospheric Pressure (APPECVD) with  
34 plasma jet and tetraethylorthosilicate (TEOS) as precursor, leading to a  $158\pm 7$  nm thickness  
35 and a 14 days stability of hydrophilic properties for a COC-embedded microchannel (100  
36  $\mu\text{m}$ ), paving the way for a simplified and controlled COC surface modification.

37 `

38

39

40

## 41 **1 Introduction**

42

43 Lab-On-A-Chip (LOAC) technology promises solutions for high throughput and highly  
44 specific analysis for environment and health applications. The choice of the material to  
45 engineer them is crucial. Indeed, each material has its own physicochemical properties which  
46 determine the microfabrication method. Moreover, it is sometimes necessary to modify the  
47 physico-chemical properties of the microchannel surface for subsequent functionalization  
48 and/or fluid flow control. Therefore, the challenge is to develop LOAC materials allowing  
49 fast, easy and cheap microfabrication methods and efficient surface treatment. Since nearly  
50 20 years poly(dimethyl siloxane) (PDMS) has been a popular material for the fabrication of  
51 microfluidic devices due to its easy microfabrication method, its elastic and transparency  
52 properties and its biocompatibility.<sup>[1,2]</sup> However, there is nowadays a move towards  
53 thermoplastic materials for their reduced cost and easier microfabrication.<sup>[3-7]</sup> Among the  
54 various thermoplastics, cyclic olefin copolymer (COC) has emerged as it offers a high  
55 chemical resistance and exhibits an optical transparency close to that of glass (for  
56 wavelengths over 300 nm).<sup>[8]</sup> COC microsystems are furthermore easily micro fabricated  
57 allowing for both rapid prototyping and low-cost mass production.<sup>[9,10]</sup>

58 Despite all these advantages, COC's main drawbacks as a material for microfluidics are its  
59 surface chemical inertness and its hydrophobic properties. In the case of LOACs, the  
60 integration of the different steps of an analytical chain (pre-concentration, separation and  
61 detection) in microchannels mainly implies a chemical modification of the COC surface.  
62 Some COC microchannel treatments provide hydrophilic properties to control electrokinetic  
63 separations<sup>[11-15]</sup> or to integrate chemical reactive groups for ligands<sup>[12,13,16-19]</sup> or monolith<sup>[20-</sup>  
64 <sup>22]</sup> immobilization. Moreover, surface functionalization of COC micro channels minimizes the  
65 adsorption of analytes in particular biological molecules.<sup>[11,14,18,23]</sup> Nowadays, three main

66 COC surface functionalization strategies are commonly used: UV/ozone oxidation,<sup>[24,25]</sup>  
67 photografting<sup>[11,13,15,20,21,23,26–29]</sup> and plasma processes<sup>[16,19,30–36]</sup>.

68 The UV/ozone oxidation procedure relies on the exposition of the COC surface under a  
69 mercury lamp and in an air-filled chamber at atmospheric pressure resulting in the generation  
70 of ozone. This treatment permits to confer hydrophilic properties to COC surfaces.<sup>[24,25]</sup>

71 Photografting is performed by a photoinitiator under a UV light, which excitation promotes  
72 abstraction of hydrogen atoms from the COC surface, leading to the formation of radicals  
73 which then initiate a surface grafting polymerization process.<sup>[37]</sup> Generally, photografting is  
74 performed through a single step, that can lead to a significant amount of ungrafted  
75 polymer.<sup>[23]</sup>

76 Plasma is widely used for COC surfaces treatment<sup>[16,19,30–35,38]</sup>, so as to shift the COC surface  
77 to a hydrophilic one, due to its oxidation, molecule chain scissions, substitution and  
78 recombination<sup>[31,38]</sup>. Several gases or gas mixtures have been extensively used for plasma  
79 generation such as oxygen, argon or nitrogen.<sup>[30–32,38]</sup> The main advantages of this surface  
80 treatment are that it is an environmentally benign process and leads to a homogeneous  
81 surface.<sup>[30–32,38]</sup>

82 One renowned plasma process to deposit chemical layer on surfaces is Plasma-Enhanced  
83 Chemical Vapor Deposition (PECVD).<sup>[39]</sup> This low-pressure plasma process consists in the  
84 fragmentation of a precursor inside gas plasma. Organosilicon-oxygen mixtures are widely  
85 used to generate thin silica film deposition, notably for microfluidic applications.<sup>[35–36]</sup> The  
86 thin silica layer confers hydrophilic properties allowing the generation of a controlled  
87 electroosmotic flow for electrokinetic separations inside COC microchannels.<sup>[40]</sup> Moreover,  
88 the presence of reactive chemical functions, such as silanol groups (SiOH), due to plasma  
89 polymerization of organosilicon precursors,<sup>[35–36]</sup> could allow the grafting of several chemical  
90 entities<sup>[41–42]</sup>. Da Silva et al. have shown the possibility to deposit by PECVD at low pressure  
91 thin layers of silica (700 nm thickness) on COC surface.<sup>[36]</sup> This layer was characterized by

92 water contact angle (WCA), X-ray photoelectron spectroscopy (XPS), Fourier-transform  
93 infrared spectroscopy (FTIR) and ellipsometry measurements, showing the presence of a  
94 silica film on the COC substrate. Ladner et al. demonstrated the activation of COC surface by  
95 a plasma at low pressure composed of 1-bromopropane as the brominated precursor and of  
96 argon gas, to create brominated functionalities that could permit to immobilize ligands  
97 through subsequent chemical modifications *via* a click chemistry reaction.<sup>[19]</sup>

98 The main drawback of many plasma treatments is the use of low pressures leading to  
99 expensive and cumbersome plasma equipments hardly adapted for industrial continuous  
100 operations.<sup>[43]</sup> Moreover, generation of a vacuum could take several hours, depending on the  
101 vacuum required, and increase the overall process time. To overcome this, plasma surface  
102 treatments were further developed at atmospheric pressure. A study has demonstrated the  
103 possibility to deposit a thin silica film in few minutes inside COC microchannels at  
104 atmospheric pressure with organosilicon precursor.<sup>[35]</sup> The silica layer was deposited with a  
105 helium-oxygen plasma generated between two electrodes integrated outside the chip and an  
106 organosilicon precursor circulating inside the COC channel.

107 This study reports, for the first time, the deposition of a silica coating inside COC  
108 microchannel with a plasma jet at atmospheric pressure. Plasma jet is advantageous over  
109 plasma treatments at atmospheric pressure proposed by Theelen et al.<sup>[35]</sup> Indeed, it does  
110 neither need the integration and the alignment of electrodes outside the chip, nor a gas flow  
111 through the microchannel, which greatly simplifies the microfabrication steps and avoids the  
112 use of several external equipments. Moreover, the plasma jet permits to treat several  
113 microchannels simultaneously in a few seconds. The experimental conditions for this COC  
114 surface modification with tetraethylorthosilicate (TEOS) were optimized so as to obtain a  
115 homogeneous density of silanol groups on its surface, for further functionalization and for the  
116 generation of an electroosmotic flow inside COC microchannels. Experimental conditions  
117 were optimized in terms of distance between the nozzle and the substrate, TEOS and carrier

118 air flow rates, and number of treatment cycles. The treatment of COC channels by the  
119 Atmospheric Pressure plasma jet proved to be fast and easily transposable for industrial  
120 applications. This process does not require complicated microfabrication steps, is  
121 environmentally friendly and will allow to design new LOACs involving COC materials.

122

## 123 **2 Materials and Chemicals**

124

125 COC plates (Topas® grade 8007,  $T_g = 75^\circ\text{C}$ , 1 mm thickness) were purchased from  
126 Microfluidic ChipShop. Brass mold (8 cm \* 8 cm \* 5 mm) was purchased from GREM  
127 (France). Silica wafers (4 inches, 500  $\mu\text{m}$  of thickness) were purchased from Prolog Semicor  
128 (Ukraine). Tetraethylorthosilicate (TEOS, 98%), was purchased from Sigma-Aldrich.  
129 2-propanol (99.9%) was purchased from GPR Rectapur. Ultra-pure water (resistivity  $\geq 18.2$   
130  $\text{M}\Omega$ , Purelab Flex, Elga Veolia, France) was used.

131

132

133

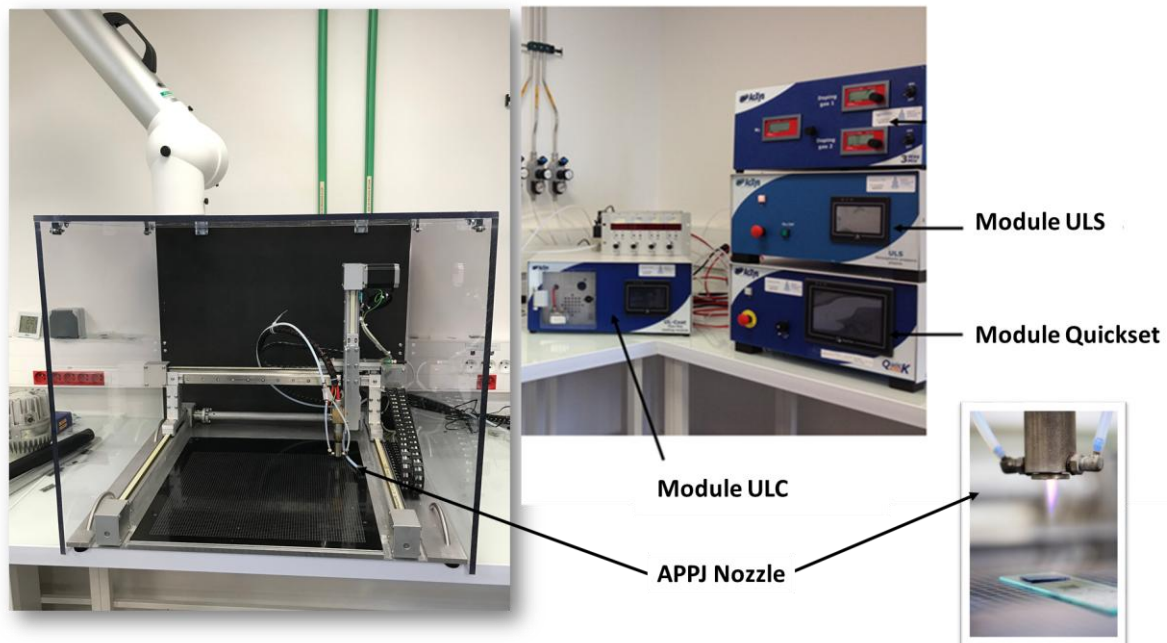
## 134 **3 General Procedure for the Silica-Like Deposition Using AcXys®**

### 135 **plasma jet on COC Surface**

136

137 In this study, the silica thin film has been deposited with an atmospheric pressure plasma  
138 system produced by AcXys® Technologies (Saint Martin le Vinoux, France). This system is  
139 composed of three command modules and a moving nozzle. The frequency is set with ULS  
140 command module where the power and the gas throughout are displayed. Thus, the APPJ  
141 (Atmospheric Pressure Plasma Jet) nozzle is mounted on a motorized xyz table (controlled  
142 using the Quickset module) so that it can sweep the surface of the sample at constant speed

143 (fixed at 150 mm/s) in order to deliver a homogeneous treatment. The plasma jet is generated  
144 by introducing air (35 L/min) into the plasma torch. The ULC module is used to inject the  
145 liquid organosilicon precursor (TEOS) contained in a pressurized tank into the treatment  
146 nozzle at a flow rate between 10  $\mu$ L/min and 500  $\mu$ L/min. The carrier gas (at a flow rate  
147 between 5 L/min and 25 L/min) vaporizes the liquid precursor which is then injected in post-  
148 discharge *via* pipes placed on each side of the nozzle. It should be noticed that the liquid  
149 precursor is controlled by a liquid flow meter before being nebulized by the venturi effect.  
150 The precursor thus nebulized is transported by the carrier gas to the deposition nozzle. The  
151 system operates at room temperature.



#### 155 **4 Microfabrication of COC Channels**

156

157 The design of channels was performed with the 3D CAO software Inventor<sup>®</sup> and then  
158 transposed on a brass mold with micro-molding technic (Minitech<sup>®</sup>). Afterwards, hot  
159 embossing was applied to COC (75 mm \* 25 mm \* 1 mm) plates, inside a 3 tons hydraulic

160 press (Scannex<sup>®</sup>) at 150°C, under a 15 bars pressure for 30 min. The system was then cooled  
161 at room temperature before shutting off the pressure. The dimensions of simple COC  
162 rectangular microchannels used during the study are of 6 cm length, 100 μm width and 30 μm  
163 height.

164

## 165 **5 Characterizations of the Silica-Like Deposition on COC Surface**

166 COC raw plates and COC treated plates are characterized by the following methods. Infrared  
167 spectra were acquired using a Fourier Transform Infrared Spectrometer (Cary 660  
168 Spectrometer, Agilent) with an Attenuated Total Reflectance module (GladiATR, Pike). The  
169 ATR-FTIR spectra were collect from 4 000 to 500 cm<sup>-1</sup>, at a resolution of 4 cm<sup>-1</sup>. 100 scans  
170 were made for each measurement. The background (air) was taken before each measurement.  
171 Static ultrapure water (resistivity ≥ 18.2 MΩ) contact angle (WCA) measurements were done  
172 thanks to a DSA25-Drop Shape Analyser from Krüss. A 2 μL droplet was released from a  
173 syringe and placed slowly on the surface which contact angle was measured after 30 s.  
174 Similar experiment were conducted on the modified material after 14 days of storage in a petri  
175 dish at room temperature and at atmospheric pressure to simulate the COC microchips storage  
176 conditions. Images of droplet formation captured using a high-resolution camera were  
177 analyzed with the Advance Image Analysis Software. The reported contact angle values are  
178 an average at least three measurements at various locations on COC plates.

179 Optical microscopy (Axio Observer A1, Zeiss) was performed with a CCD digital camera  
180 (Pike F145B, Allied Vision Technologies Stadtroda, Germany) and an image acquisition  
181 software (Hiris, RD Vision, France). Images were reprocessed *via* Image J software.

182 Spectroscopic ellipsometry (UVISEL, Horiba Jobin Yvon) was performed at an incidence  
183 angle of 60°, with a 75 W Xe lamp over a spectral range of 245±2100 nm (i.e., 0.6±5 eV).

184 Ellipsometry is based on variation of light polarization, which is reflected by the sample.<sup>[44]</sup>

185 As COC substrates do not reflect light,<sup>[8]</sup> a silica wafer was chosen as model substrate to

186 determine the thickness of silica deposits<sup>[19]</sup>. The reported thickness values are an average of  
187 at least three measurements at various locations on modified of plate surfaces.

188

## 189 **6 Results and Discussion**

190

191 As a preliminary treatment, COC plates were sonicated in isopropanol and then water (during  
192 3 min). When treated with the plasma jet, COC plates were attached with carbon tape on a  
193 holder. So as to remove eventual low molecular weight fragments at the topmost COC surface  
194 layer,<sup>[36]</sup> they were pre-treated by Air Plasma at Atmospheric Pressure (APAP) at 80 kHz (987  
195 W, 35 L/min air) with a nozzle speed of 150 mm/s. Indeed, oxygen radicals and excited  
196 molecules produce volatile organic and inorganics compounds such as CO, CO<sub>2</sub>, H<sub>2</sub>O  
197 molecules, eliminating low molecular weight oxidized fragments. In a second step, a silica  
198 film was then deposited on COC surfaces by APPECVD process, under an air plasma to  
199 decompose TEOS 80 kHz (1030 W, 35 L/min air) with a nozzle speed of 150 mm/s. The  
200 APPECVD process could be applied several times, “a treatment cycle” being defined as one  
201 APPECVD process.

202 The influence of several experimental parameters on the silica coating of COC substrates (2  
203 cm<sup>2</sup>) was studied. These parameters are the distance between the nozzle and the substrate  
204 surface (from 16.5 to 31.5 mm), the TEOS flow rate (from 100 µL/min to 200 µL/min), the  
205 carrier air flow rate (from 5 to 20 L/min), and the number of treatment cycles (from 1 to 5).  
206 The COC plates before treatment, after the APAP step, and after APAP + APPECVD were  
207 characterized by ATR-FTIR, WCA and optical microscopy. The thickness of silica layers was  
208 measured by ellipsometry.

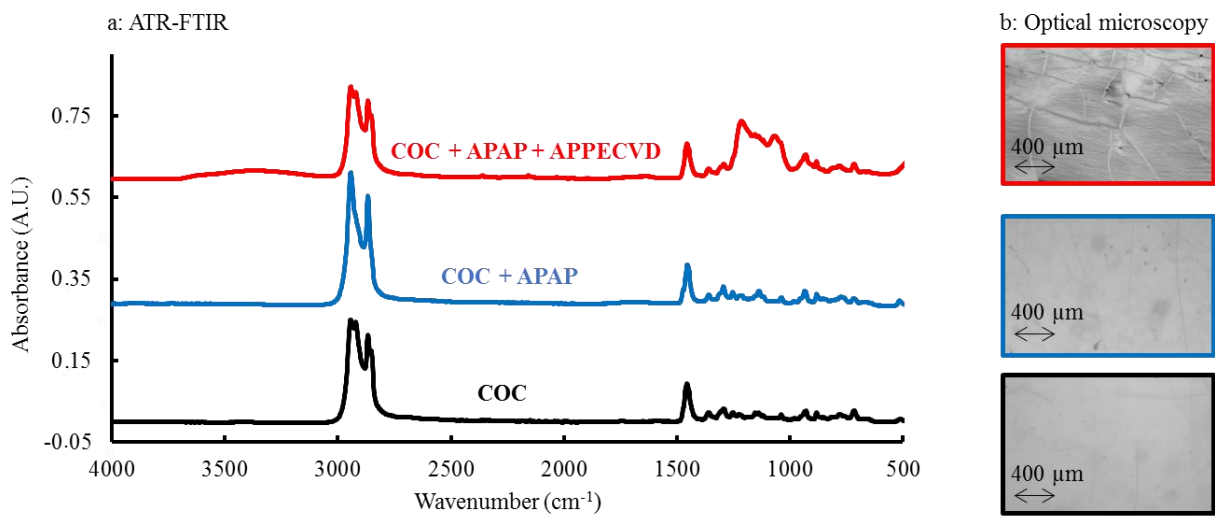
209

210

### 211 **6.1 Characterizations of Untreated and Plasma Treated COC Plates**

212

213 Figure 2 shows ATR-FTIR (**Figure 2.a**) and optical microscopy characterizations (**Figure**  
214 **2.b**) of COC surfaces, either before any treatment, after APAP treatment and after APAP+  
215 one APPECVD cycle. The water contact angle measurements were done for each step of the  
216 silica deposit process. The thickness of the silica layer after APPECVD treatment was also  
217 measured.



218

219 *Figure 2. COC substrate characterizations before any treatment (bottom graph and image),*  
220 *after APAP treatment (middle graph and image) and after APAP + APPECVD treatments*  
221 *(upper graph and image) by (a) ATR-FTIR, and (b) optical microscopy. Experimental*  
222 *conditions for APAP: 16.5 mm between torch and surface and 150 mm/s nozzle speed (~300*  
223 *ms treatment time). Experimental conditions for APPECVD: 16.5 mm between torch and*  
224 *surface, 200 μL/min TEOS, 5 L/min carrier air and 150 mm/s nozzle speed (~300 ms*  
225 *treatment time).*

226

227 Untreated COC surfaces present an ATR-FTIR spectrum (**Figure 2.a**) with absorption bands  
228 located at 2947 and 2868 cm<sup>-1</sup> which are assigned to carbon/hydrogen stretching vibration  
229 modes of -CH<sub>2</sub> and -CH<sub>3</sub> groups from the polymer backbone. The band around 1456 cm<sup>-1</sup>  
230 corresponds to the wagging mode of -CH<sub>3</sub> groups.<sup>[36]</sup> The WCA measurements of untreated  
231 COC plate (95±1°) confirmed the hydrophobic properties of the polymer.<sup>[8]</sup> Optical

232 microcopy characterization showed that the COC surface was transparent and homogeneous  
233 (**Figure 2.b**).<sup>[8]</sup>

234

235 The ATR-FTIR spectrum of APAP-treated COC surface did not present any difference with  
236 that of the untreated COC surface (**Figure 2.a**). After APAP treatment, the WCA values  
237 dropped from  $95\pm 1^\circ$  to  $48\pm 7^\circ$ . This can be explained by the insertion of polar functional  
238 groups onto the surface of the raw hydrophobic COC substrate after APAP  
239 treatment,<sup>[30,33,34,38,45]</sup> leading to a more hydrophilic surface. ATR-FTIR spectroscopy is not  
240 sensitive enough to detect the presence of polar groups deposited by APAP treatment. Roy et  
241 al. have suggested a possible reaction mechanism on COC surface during plasma  
242 treatment<sup>[38]</sup>, the electrons, ions and free radicals generated during high energy plasma  
243 irradiation promoting breakage of the C-H and C-C bonds. This would lead to shorter polymer  
244 carbon chain, the formation of other molecules through recombination reaction and also  
245 crosslinking.<sup>[38]</sup> As nitrogen and oxygen atoms are present, chemical interactions between the  
246 radicals from air and thermoplastics occur, which promote the insertion of polar groups like  
247 hydroxyl, ketone or carboxylic acid for example.<sup>[32]</sup> Optical microcopy characterization  
248 showed that APAP-treated COC surface did not present any difference compared to untreated  
249 COC (**Figure 2.b**). APAP treatment preserved the optical transparency of the substrate.

250

251 After APPECVD treatment, three new ATR-FTIR bands appeared in addition to the  
252 characteristic bands of COC backbone. During APPECVD treatment, a silica layer was  
253 deposited due to the reaction between oxygen reactive atoms and the precursor, generating  
254 emission of carbon dioxide and water.<sup>[36]</sup> The two bands at  $1225\text{ cm}^{-1}$  and  $1078\text{ cm}^{-1}$   
255 correspond to the Si-O-Si asymmetrical and symmetrical stretching modes, respectively.<sup>[36,46]</sup>  
256 The band located at  $3342\text{ cm}^{-1}$  is assigned to hydroxyl group (stretching mode). This band is  
257 related to the presence of Si-OH groups, as the interaction between the  $-\text{SiO}_2$  layer and the air

258 leads to the formation of –OH groups at the outer surface of the coating.<sup>[36]</sup> The initial bands  
259 originating from the COC thermoplastic backbone (2947, 2868 and 1456 cm<sup>-1</sup>) were still  
260 present due to the low thickness of the silica layer (39±5 nm) compared to the depth to the  
261 analysis .<sup>[36]</sup> The WCA values dropped from 48±7° to 27±2° for APAP- and APAP +  
262 APPECVD-treated COC surface, respectively, evidencing the deposition of a more  
263 hydrophilic layer. Optical microscopy characterization shows that APPECVD treatment  
264 induced micro-cracked surface layer (**Figure 2.b**).

265 In order to generate a homogeneous immobilization of ligands/monoliths or a repeatable  
266 electroosmotic flow between various batches of COC LOACs, the surface layer should be as  
267 homogeneous as possible. Micro-cracks may be due to the generation of an elevated  
268 temperature during plasma treatment that could degrade the surface. By increasing the  
269 distance between the nozzle and the substrate, temperature during the treatment should be  
270 lowered.

271

## 272 **6.2 Influence of the Distance Between the nozzle and the Surface on the Silica**

### 273 **Coating**

274

275 To avoid the presence of cracks evidenced on APAP + APPECVD-treated COC surface,  
276 probably caused by a too high treatment temperature process, the distance between the torch  
277 and the substrate was increased, step by step (by 5 mm), from 16.5 mm and 31.5 mm. The  
278 increase in this distance should allow reducing the temperature during the treatment. The  
279 study was performed in the same experimental conditions as previously described except for  
280 the distance between the torch and the substrate. For each distance, the thickness of the silica  
281 layer was measured by ellipsometry and the presence of cracks was checked by optical  
282 microscopy (Table 1).

283

284 *Table 1. Influence of the distance between the torch and the COC surface on the silica layer*  
 285 *thickness determined by ellipsometry. For experimental conditions for silica deposition, see*  
 286 *Figure 2.*

<b>Distance between the torch and the surface of the substrate [mm]</b>	<b>Silica coating thickness [nm]</b>	<b>Presence of cracks</b>
16.5	39±5	Yes
21.5	43±11	Yes
26.5	38±8	Yes
31.5	20±3	No

287

288 When torch/substrate distance was increased, the silica layer thickness decreased  
 289 concomitantly. This can be explained by the fact that, air/TEOS plasma spot reaches the COC  
 290 surface with a large diameter, leading to less TEOS reactive species density onto the COC  
 291 surface. The cracks were no more visible when applying a distance of 31.5 mm. For all the  
 292 tested distances, the wettability did not change, with a constant value of ~30°.

293

294

295

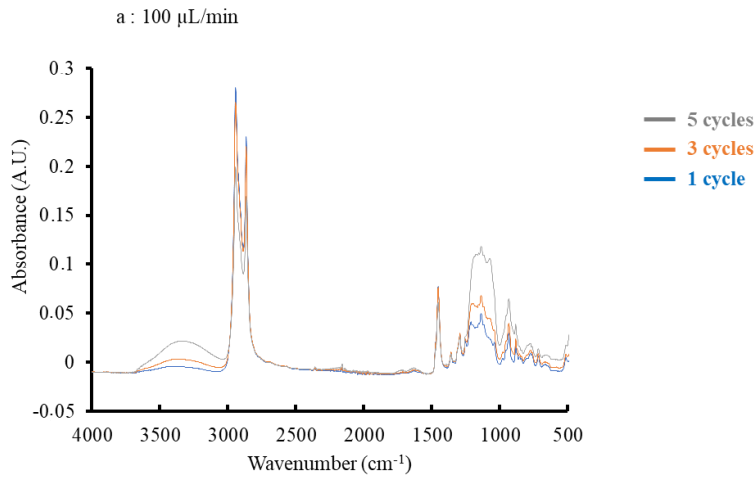
296

### 297 **6.3 Influence of the TEOS flow rate and number of treatment cycles**

298

299 The influence of the TEOS flow rate (100 and 200 µL/min) and the number of treatment  
 300 cycles (1, 3 and 5) on the properties of the deposited silica layer were studied by ATR-FTIR,  
 301 WCA and ellipsometry (**Figure 3**). For this study, the carrier air flow rate was fixed at its high  
 302 value (20 L/min) to consider a high silica and silanol density, for a better sensitivity with  
 303 ATR-FTIR measurements.

304



305

306

307

308

309

310

311

312

313

Treatment cycles	WCAs ( $^{\circ}$ )	Silica coating thickness (nm)
1 cycle	32 $\pm$ 1	37 $\pm$ 6
3 cycles	24 $\pm$ 2	43 $\pm$ 2
5 cycles	<10 $\pm$ 0	74 $\pm$ 4

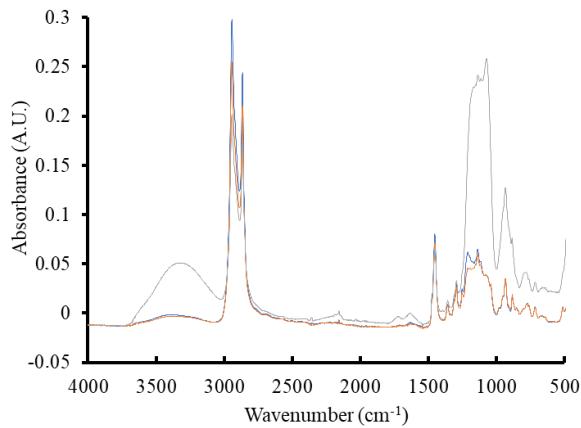
314

315

316

317

b : 200  $\mu\text{L}/\text{min}$



318

319

320

321

322

323

Treatment cycles	WCAs ( $^{\circ}$ )	Silica coating thickness (nm)
1 cycle	36 $\pm$ 1 $^{\circ}$	44 $\pm$ 2 nm
3 cycles	16 $\pm$ 3 $^{\circ}$	87 $\pm$ 4 nm
5 cycles	<10 $\pm$ 0 $^{\circ}$	158 $\pm$ 7 nm

324

325

326

327 *Figure 3. COC substrate characterizations (ATR-FTIR, WCA and ellipsometry) after the*

328 *overall plasma treatment: (APAP followed by 1 (~300 ms), 3 (~900 ms) or 5 (~1.5 s)*

329 *APPECVD treatment cycles. Experimental conditions for APAP pre-treatment: 31.5 mm*

330 *between torch and surface, 1 cycle treatment (300 ms). Experimental conditions for*

331 *APPECVD: 31.5 mm between torch and surface, (a) 100 or (b) 200  $\mu\text{L}/\text{min}$  of TEOS and 20*

332 *L/min of carrier air flow rate.*

333 For each TEOS flow rate, the peak intensities attributed to the silica thin film (3342, 1225 and  
334 1078  $\text{cm}^{-1}$ ) increased with the number of treatment cycles. On the other side, peak intensities  
335 originating from the thermoplastic backbone (2947, 2868 and 1456  $\text{cm}^{-1}$ ) decreased when  
336 increasing the number of cycles (**Figure 3**). These results are consistent with an increase in  
337 silica deposit with the number of cycles. These results furthermore indicate that wettability  
338 increased with the number of treatment cycles. Concerning ellipsometry measurements, the  
339 layer thickness was confirmed to increase with the number of treatment cycles.  
340 Moreover, the TEOS flow rate played a key role on the silica layer characteristics. The  
341 intensity of the band attributed to -OH groups from silanol (3342  $\text{cm}^{-1}$ ) was twice higher at  
342 200  $\mu\text{L}/\text{min}$  (5 cycles) compared to 100  $\mu\text{L}/\text{min}$  (5 cycles) of flow rate (**Figure 3**). The higher  
343 the flow rate, the more hydrophilic the treated surface and the thicker the layer. This result is  
344 in accordance with previous studies.<sup>[47]</sup> So a higher silica density was deposited with the  
345 higher TEOS flow rate on COC surface. Optical microscopy characterizations were done to  
346 verify the absence of visible cracks with all combinations of experimental conditions tested.  
347 For all of them, no crack on the surface treated by APAP + APPECVD were noticed (data not  
348 shown).

349

350

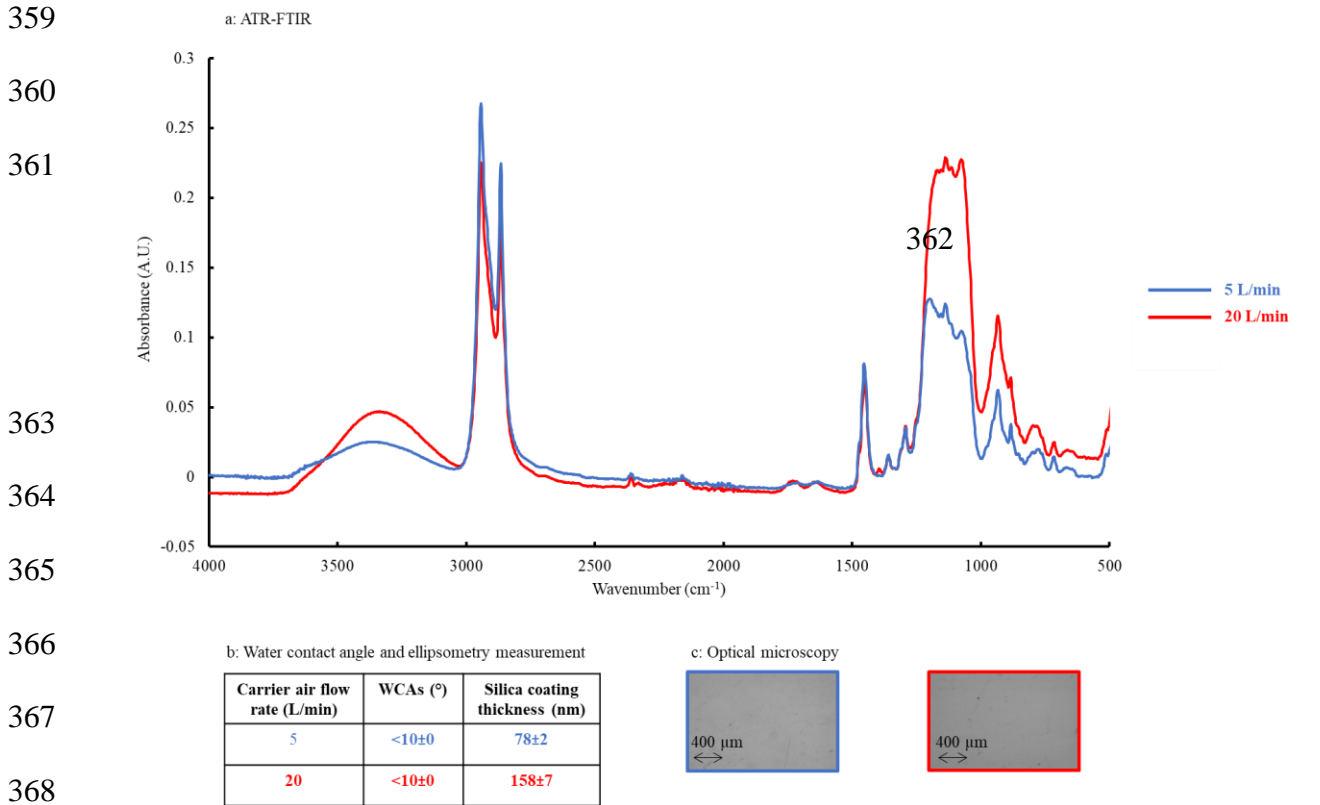
#### 351 **6.4 Influence of the Carrier Air Flow Rate**

352

353 Another experimental parameter for the optimization of the silica layer is the carrier air flow  
354 rate, which was varied from 5 to 20 L/min. For each flow rate, ATR-FTIR, WCA and  
355 ellipsometry measurements were performed and the presence of cracks was checked by  
356 optical microscopy (**Figure 4**).

357

358



369 *Figure 4. COC substrate characterizations by (a) ATR-FTIR, (b) WCA and ellipsometry, and*  
 370 *(c) optical microscopy after APAP and 5 APPECVD treatment cycles. Experimental*  
 371 *conditions for APAP pre-treatment: 31.5 mm between torch and surface, 1 cycle (300 ms).*  
 372 *Experimental conditions for APPECVD: 31.5 mm between torch and surface, 200 μL/min of*  
 373 *TEOS, 5 treatment cycles (1.5 s) and 5 (blue) or 20 L/min (red) of carrier air flow rate.*

374  
 375 ATR-FTIR spectra indicate that the absorbance of the bands attributed to the silica layer  
 376 (3342, 1225 and 1078 cm<sup>-1</sup>) increased with the carrier air flow rate, whereas the absorbance of  
 377 the bands originating from the thermoplastic backbone (2947, 2868 and 1456 cm<sup>-1</sup>) decreased  
 378 (**Figure 4.a**). The thickness of the silica layer increased from 78±2 nm to 158±7 nm, when the  
 379 carrier air flow increased from 5 L/min to 20 L/min (**Figure 4.b**). It therefore seems that the  
 380 increase in carrier air flow leads to higher silanol density on plasma treated COC  
 381 thermoplastic (**Figure 4.a and 4.b**). This can be explained by an increase in interaction  
 382 between SiO<sub>2</sub> layer and the air, as reported in the literature.<sup>[38]</sup> With 5 L/min and 20 L/min  
 383 carrier air flow rates, the optical characterizations of the surface proved the absence of crack

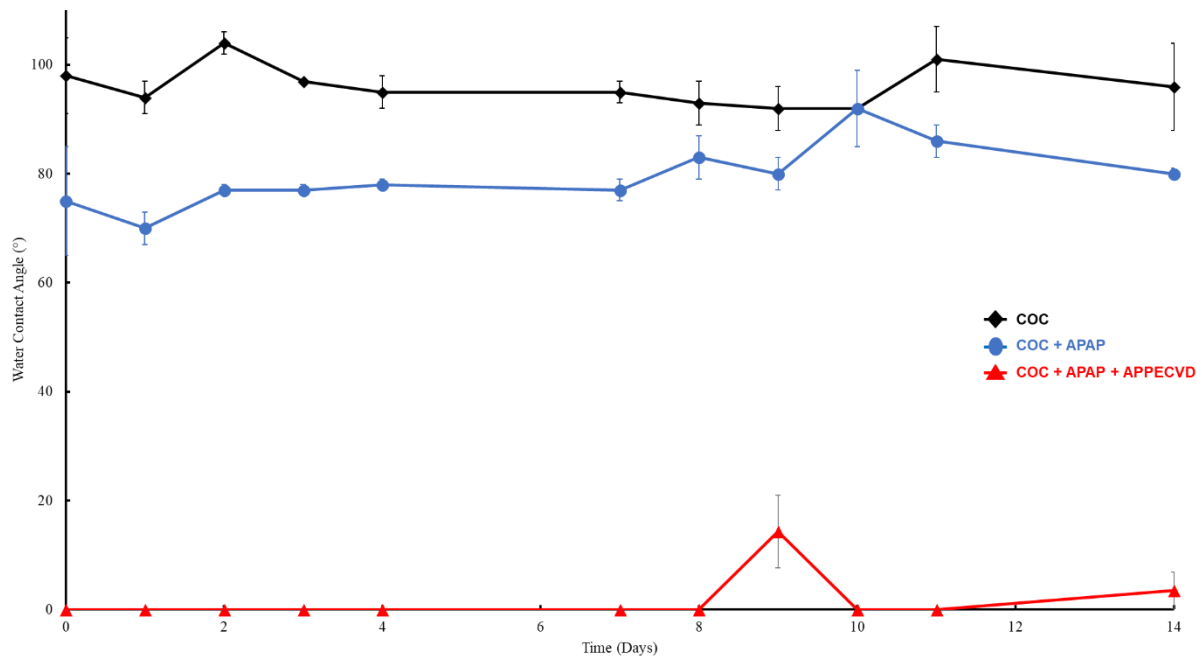
384 on the silica deposit (**Figure 4.c**). Therefore, the objective to obtain a sufficient and  
385 homogeneous surface silanol density for further functionalization<sup>[41-42]</sup> can be reached with the  
386 following APPECVD conditions: a 31.5 mm distance between the torch and the surface, 200  
387  $\mu\text{L}/\text{min}$  TEOS flow rate, 20 L/min carrier air flow rate and 5 treatment cycles. This COC  
388 surface modification should allow the generation of a controlled electroosmotic flow inside  
389 COC microchannels<sup>[40]</sup>. The silica layer was then of  $158 \pm 7$  nm thickness with a contact angle  
390 of less than  $10^\circ$ . These performances are similar to the ones of other plasma processes on  
391 COC surfaces for silica deposition in terms of layer thickness (between  $250 \text{ nm}^{[35]}$  and  $700$   
392  $\text{nm}^{[36]}$  for atmospheric pressure and low pressure plasma respectively) and wettability ( $\sim 10^\circ$ ).  
393 The plasma process described herein relies on simplified conditions in terms of equipments,  
394 treatment rapidity and costs<sup>[41]</sup> and allows generating the deposition of a silica layer on COC  
395 surface with a similar wettability and the same order of magnitude for the silica layer  
396 thickness (between 100 and 900 nm) as the plasma process at low pressure

397

## 398 **6.5 Stability of the Silica Layer**

399

400 The stability of the silica layer deposited using the optimized experimental conditions  
401 (APPECVD: 31.5 mm between torch and surface, 200  $\mu\text{L}/\text{min}$  TEOS flow rate, 20 L/min  
402 carrier air flow rate and 5 treatment cycles) was studied by WCA measurements. APAP +  
403 APPECVD-treated COC plate was stored in a petri-dish at room temperature and at  
404 atmospheric pressure for 14 days to simulate the COC microchips storage conditions. As a  
405 matter of comparison, untreated COC surface and APAP-treated COC plates were stored and  
406 studied under the same conditions (**Figure 5**).



407  
 408 *Figure 5. Evolution of WCA measurements in function of storage time (0 to 14 days) for raw*  
 409 *(COC), pre-treated with APAP (COC + APAP) and fully treated (COC + APAP +*  
 410 *APPECVD) COC surface. Storage conditions: in petri-dish at atmospheric pressure and*  
 411 *room temperature. Experimental conditions for APAP: 31.5 mm between torch and surface*  
 412 *and 1 cycle (300 ms). Experimental conditions for APPECVD: 31.5 mm between torch and*  
 413 *surface, 200  $\mu$ L/min TEOS flow rate, 20 L/min carrier air flow rate and 5 treatment cycles*  
 414 *(1.5 s).*

415  
 416 As shown in **Figure 5**, silica layers deposited on COC surface are stable over 14 days, in  
 417 accordance with another study.<sup>[36]</sup> The COC plates with a APAP + APPECVD plasma  
 418 treatment can thus be stored during 2 weeks at atmospheric pressure and room temperature  
 419 before further processing.

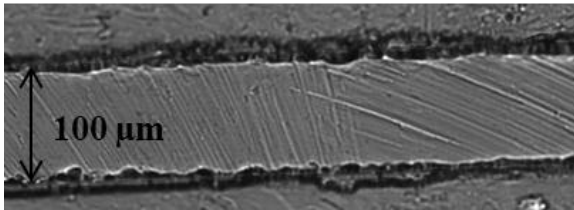
420  
 421 **6.6 Optical Characterization of Plasma Treated COC Microchannels**

422  
 423 So as to evaluate the transposition of our process into COC microchannels, preliminary  
 424 experiments were conducted using optimized conditions for silica coating in single COC

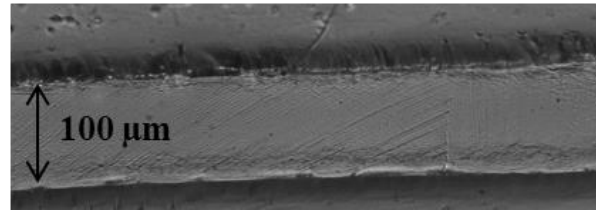
425 microchannels of 6 cm length, 100  $\mu\text{m}$  width and 30  $\mu\text{m}$  height. Optical characterizations of  
426 COC microchannels were performed before and after APAP + APPECVD treatment, as  
427 illustrated in Figure 6.

428

a : Before silica coating



b : After silica coating



429

430 *Figure 6. Optical characterizations of COC microchannels (a) before and after (b) silica*  
431 *coating by plasma treatment at atmospheric pressure. Experimental conditions for APAP and*  
432 *APPECVD: see Figure 5. Fully treatment time (COC + APAP + APPECVD) microchannel is*  
433 *~2.4 s. The black line is 100  $\mu\text{m}$  bar scale.*

434

435 This figure shows that scratches inside COC microchannel due to the brass mold can be  
436 observed (Fig 6 a). After APAP + APPECVD treatment, almost all scratches disappeared,  
437 probably screened by the deposition of a thin silica layer into the microchannel (**Figure 6.b**).  
438 The thin silica layer overlaid the defects inside COC microchannels. These results prove the  
439 efficient transposition of the *in situ* plasma process, inside microdevices.

440

441

442

443

## 444 **7 Conclusion**

445

446 This study reports for the first time a new plasma process for simplified, quick and efficient  
447 silica layer deposition on COC surfaces. This new procedure employs Plasma-Enhanced  
448 Chemical Vapor Deposition at Atmospheric Pressure (APPECVD) with a plasma jet, TEOS  
449 as precursor and air gas. The optimization of different experimental conditions allowed to  
450 generate a homogeneous silica coating on COC surface. The optimal experimental conditions  
451 permitted to deposit a  $158\pm 7$  nm hydrophilic silica layer that proved to be stable over 14 days  
452 stored at room temperature and atmospheric pressure.

453 This fast and versatile plasma process compared to the ones generated at low pressure,  
454 allowed to deposit thin silica layers of similar properties on COC substrate. This plasma jet  
455 treatment also allowed *in situ* treatment of COC microchannels, that is to say fast and easy  
456 microfabrication process of the microchips, is environmentally friendly and can be further  
457 used for industrial application, among which the production of COC LOAC.

458 Acknowledgements: Ecole Doctorale 406 (PSL and Sorbonne Université) is acknowledged  
459 for its financial support. This work has received the technical support of "Institut Pierre-Gilles  
460 de Gennes" (laboratoire d'excellence, "Investissements d'avenir" program ANR-10-IDEX-  
461 0001-02 PSL and ANR-10-LABX-31.).

462

463 Received: ((will be filled in by the editorial staff)); Revised: ((will be filled in by the editorial  
464 staff)); Published online: ((please add journal code and manuscript number, e.g., DOI:  
465 10.1002/ppap.201100001))

466

467 Keywords: APPECVD; COC; silica coated; TEOS; microfluidic.

468

469

470 [1] Y. Xia and G. M. Whitesides, *Angew. Chem. Int. Ed.* **1998**, *37*, 550.

471 [2] J. Zhou, A. V. Ellis and N. H. Voelcker, *Electrophoresis* **2010**, *31*, 2.

- 472 [3] T. B. Stachowiak, F. Svec and J. M. Fréchet, *J. Chromatogr. A.* **2004**, *1044*, 97.
- 473 [4] K. Faure, *Electrophoresis* **2010**, *31*, 2499.
- 474 [5] M. Pumera, *Talanta* **2005**, *66*, 1048.
- 475 [6] D. Wu, J. Qin and B. Lin, *J. Chromatogr. A.* **2008**, *1184*, 542.
- 476 [7] K. Ren, J. Zhou and H. Wu, *Acc. Chem. Res.* **2013**, *46*, 2396.
- 477 [8] P. S. Nunes, P. D. Ohlsson, O. Ordeig and J. P. Kutter, *Microfluid. Nanofluidics* **2010**, *9*,
- 478 145.
- 479 [9] R. Novak, N. Ranu and R. A. Mathies, *Lab. Chip* **2013**, *13*, 1468.
- 480 [10] U. M. Attia, S. Marson and J. R. Alcock, *Microfluid. Nanofluidics* **2009**, *7*, 1.
- 481 [11] C. Li, Y. Yang, H. G. Craighead and K. H. Lee, *Electrophoresis* **2005**, *26*, 1800.
- 482 [12] A. Muck and A. Svatos, *Talanta*, DOI:10.1016/j.talanta.2007.09.012.
- 483 [13] Q. Pu, O. Oyesanya, B. Thompson, S. Liu, and J. C. Alvarez, *Langmuir* **2007**, *23*,
- 484 1577.
- 485 [14] J. Zhang, C. Das and Z. H. Fan, *Microfluid. Nanofluidics* **2008**, *5*, 327.
- 486 [15] S. Roy, T. Das and C. Y. Yue, *ACS Appl. Mater. Interfaces* **2013**, *5*, 5683.
- 487 [16] C. Jönsson, M. Aronsson, G. Rundström, C. Pettersson, I. Mendel-Hartvig, J. Bakker,
- 488 E. Martinsson, B. Liedberg, B. MacCraith, O. Öhman and J. Melin. *Lab. Chip* **2008**, *8*,
- 489 1191.
- 490 [17] J. Raj, G. Herzog, M. Manning, C. Volcke, B. D. MacCraith, S. Ballantyne, M.
- 491 Thompson, D. W. M. Arrigan, *Biosens. Bioelectron.* **2009**, *24*, 2654.
- 492 [18] D. Sung, D. H. Shin and S. Jon, *Biosens. Bioelectron.* **2011**, *26*, 3967.
- 493 [19] Y. Ladner, F. d'Orlyé, C. Perréard, B. Da Silva, C. Guyon, M. Tatoulian, S. Griveau,
- 494 F. Bedioui and A. Varenne, *Plasma Process. Polym.* **2013**, *10*, 959.
- 495 [20] T. B. Stachowiak, D. A. Mair, T. G. Holden, L. J. Lee, F. Svec, J. M. J. Fréchet,
- 496 *Electrophoresis* **2003**, *24*, 3689.

- 497 [21] K. Faure, M. Albert, V. Dugas, G. Crétier, R. Ferrigno, P. Morin and J.-L. Rocca,  
498 *Electrophoresis* **2008**, *29*, 4948.
- 499 [22] J. Liu, C.-F. Chen, C.-W. Tsao, C.-C. Chang, C.-C. Chu and D. L. DeVoe, *Anal.*  
500 *Chem.* **2009**, *81*, 2545.
- 501 [23] T. B. Stachowiak, D. A. Mair, T. G. Holden, L. J. Lee, F. Svec and J. M. Fréchet, *J.*  
502 *Sep. Sci.* **2007**, *30*, 1088.
- 503 [24] C. W. Tsao, L. Hromada, J. Liu, P. Kumar and D. L. DeVoe, *Lab. Chip* **2007**, *7*, 499.
- 504 [25] A. Bhattacharyya and C. M. Klapperich, *Lab. Chip* **2007**, *7*, 876.
- 505 [26] S. Roy, C. Y. Yue, S. S. Venkatraman and L. L. Ma, *J. Mater. Chem.* **2011**, *21*, 15031.
- 506 [27] R. K. Jena, C. Y. Yue and L. Anand, *Sens. Actuators B Chem.* **2011**, *157*, 518.
- 507 [28] Y. Ladner, A. Bruchet, G. Crétier, V. Dugas, J. Randon and K. Faure, *Lab. Chip* **2012**,  
508 *12*, 1680.
- 509 [29] Y. Ladner, G. Crétier and K. Faure, *Electrophoresis* **2012**, *33*, 3087.
- 510 [30] S.-J. Hwang, M.-C. Tseng, J.-R. Shu and H. Her Yu, *Surf. Coat. Technol.* **2008**, *202*,  
511 3669.
- 512 [31] S. Roy and C. Y. Yue, *Plasma Process. Polym.* **2011**, *8*, 432.
- 513 [32] B.-Y. Xu, X.-N. Yan, J.-J. Xu and H.-Y. Chen, *Biomicrofluidics* **2012**, *6*, 016507.
- 514 [33] B. Cortese, M. C. Mowlem and H. Morgan, *Sens. Actuators B Chem.* **2011**, *160*, 1473.
- 515 [34] D. Nikolova, E. Dayss, G. Leps and A. Wutzler, *Surf. Interface Anal.* **2004**, *36*, 689.
- 516 [35] M. Theelen, D. Habets, L. Staemmler, H. Winands and P. Bolt, *Surf. Coat. Technol.*  
517 **2012**, *211*, 9.
- 518 [36] B. Da Silva, M. Zhang, G. Schelcher, L. Winter, C. Guyon, P. Tabeling, D. Bonn and  
519 M. Tatoulian, *Plasma Process. Polym.* **2017**, *14*, 1600034.
- 520 [37] B. Rånby, W. T. Yang and O. Tretinnikov, *Nucl. Instrum. Methods Phys. Res. Sect. B*  
521 *Beam Interact. Mater. At.* **1999**, *151*, 301.

- 522 [38] S. Roy, C. Y. Yue, Y. C. Lam, Z. Y. Wang and H. Hu, *Sens. Actuators B Chem.* **2010**,  
523 150, 537.
- 524 [39] D. Merche, N. Vandecasteele and F. Reniers, *Thin Solid Films* **2012**, 520, 4219.
- 525 [40] D. Belder and M. Ludwig, *Electrophoresis* **2003**, 24, 3595.
- 526 [41] I. M. El-Nahhal and N. M. El-Ashgar, *J. Organomet. Chem.* **2007**, 692, 2861.  
527
- 528 [42] J. Křenková and F. Foret, *Electrophoresis* **2004**, 25, 3550.  
529
- 530 [43] M. J. Shenton and G. C. Stevens, *Journal Of Physics D: Applied Physics* **2001**, 34,  
531 2761.
- 532 [44] E. Passaglia, R. R. Stromberg and J. Kruger, in *Ellipsometry in the Measurement of*  
533 *Surfaces and Thin Films: Symposium Proceedings*, U.S. National Bureau of Standards,  
534 **1964**.
- 535 [45] R. A. Lawton, C. R. Price, A. F. Runge, W. J. Doherty and S. S. Saavedra, *Colloids*  
536 *Surf. Physicochem. Eng. Asp.* **2005**, 253, 213.
- 537 [46] K.-S. Ma, F. Reza, I. Saaem and J. Tian, *J. Mater. Chem.* **2009**, 19, 7914.
- 538 [47] B. Twomey, D. Dowling, G. Byrne, L. O'Neill and L.-A. O'Hare, *Plasma Process.*  
539 *Polym.* **2007**, 4, S450.
- 540